J. COMBIN. MATH. COMBIN. COMPUT. 124 (2025) 303–315

Journal of Combinatorial Mathematics
and Combinatorial Computing
www.combinatorialpress.com/jcmcc

Combinatorial Press

Meteorological analysis based on cloud radar data acquisition and computerized data fusion techniques

Yaping Fu[1], Fang Li[2,✉], Bin Wen[3], Jingjing Li[1], Zichen Pei[1], Chen Zhao[1]

[1] *Shanxi Provincial Atmospheric Detection Technology Support Center, Taiyuan, Shanxi, 030002, China*
[2] *Shanxi Province Meteorological Society, Taiyuan, Shanxi, 030002, China*
[3] *Chengdu University of Information Technology, Chengdu, Sichuan, 610200, China*

ABSTRACT

With the frequent occurrence of global climate change and extreme weather events, meteorological forecasting technology has gradually become an auxiliary technology for production activities. In order to improve the quality of meteorological analysis results, a technology utilizing cloud radar data as the core is proposed. The vertical distribution of water vapor and liquid water in the atmosphere is detected by a ground-based microwave radiometer. The median filtering method is used to further smooth the classified and preliminarily removed reflectance factor data, and computer information processing technology is used for data analysis. The experimental results of Taiyuan ground based remote sensing high altitude detection experiment showed that in the data availability test, the research method had a data availability rate of 97.3% when the height was 2km in humidity data. When conducting accuracy analysis of the results, the root mean square error of the relative humidity profile was only 22.0% when the height increased to 12km. This indicates that the research method can conduct high-quality meteorological analysis and provide assistance for meteorological forecasting.

Keywords: cloud radar, data fusion, neural network, meteorological analysis, temperature profile

1. Introduction

Meteorological data are of vital importance to our understanding and prediction of weather and climate, as well as to our response to various weather-related activities. With the continuous development of science and technology, the sources of meteorological data are becoming more and more

✉ Corresponding author.
E-mail address: 13935165093@163.com (F. Li).

Received 02 September 2024; Accepted 10 December 2024; Published Online 17 March 2025.

DOI: 10.61091/jcmcc124-21

diversified, including satellites, radars, ground observatories, sounders, etc. [9, 15, 4, 19]. However, these different sources of data often have different characteristics and accuracy, in order to understand the meteorological situation more comprehensively and accurately, meteorological data fusion technology has emerged. Meteorological data fusion is a method of comprehensive processing and analysis of meteorological information from multiple data sources [1, 21, 13, 7]. Its purpose is to integrate data from different sources to obtain more complete, more accurate and more representative meteorological information. The realization of this technique is not simply adding or averaging the data, but needs to take into account the quality of the data, spatial and temporal resolution, error characteristics and other factors [14, 6, 22, 10].

Meteorological radar is a major tool used to monitor rainfall and meteorological phenomena. By observing the radar images, the rainfall situation in each area can be obtained, and the future meteorological trends can also be analyzed to provide basic data for weather forecasting [17, 3, 18, 8]. The working principle of meteorological radar is to utilize the scattering and reflection of RF signals, and by calculating the time, frequency, and phase of the RF signals, we can obtain the reflected signal strength and morphological information of each location in the sky [5, 16, 20, 24]. By processing and analyzing the data from multiple radars, more accurate rainfall and weather trend prediction results can be obtained. The application of weather radar data is very wide. At present, weather radar data have been widely used in weather forecasting, hydrological forecasting, transportation, aerospace, agricultural production and other fields [11, 12, 23, 2].

In this context, the research attempts to innovatively optimize data sources through data fusion based on cloud radar data. Then, combining BP neural network for high-quality analysis of meteorological conditions, it is expected to provide certain technical support for the meteorological industry.

2. Methodology

2.1. Design of data collection and quality control methods for meteorological analysis

Accurate meteorological forecasting relies on precise monitoring of the weather system, where key data collection can help meteorological professionals predict weather trends. However, meteorological phenomena vary greatly at different time and spatial scales, making high-resolution monitoring difficult. Moreover, there are differences in accuracy and types of data collected by different data collection methods. Cloud radar can obtain detailed information about clouds by emitting radar waves and receiving signals reflected back from water droplets or ice crystals in the cloud layer. Cloud radar is one of the core data sources used to construct data collection methods for meteorological analysis technology. In order to collect more comprehensive meteorological parameters as much as possible, a comprehensive collection system for meteorological analysis data is established based on cloud radar, as shown in Figure 1.

As shown in Figure 1, the comprehensive acquisition system established in the study includes a 35GHz cloud radar, ground-based microwave radiometer, and sounding equipment. The cloud radar emits radar waves and receives signals reflected back from water droplets or ice crystals in the cloud layer, obtaining the vertical structure of the cloud and tracking its development process in real time. Based on the vertical profile information provided by cloud radar, ground-based microwave radiometers detect the vertical distribution of water vapor and liquid water in the atmosphere, while sounding equipment calibrates the data from cloud radar and microwave radiometers. The microwave

radiometer provides continuous time series data, filling the gap between each launch of the sounding equipment. However, the data collection equipment itself has noise, and there may also be animals and suspended solids in the detected area, which may affect the quality of the data and require data quality control. This study uses computers to classify reflectance factor data in order to eliminate invalid data. The texture representation of echo intensity is shown in Eq. (1);

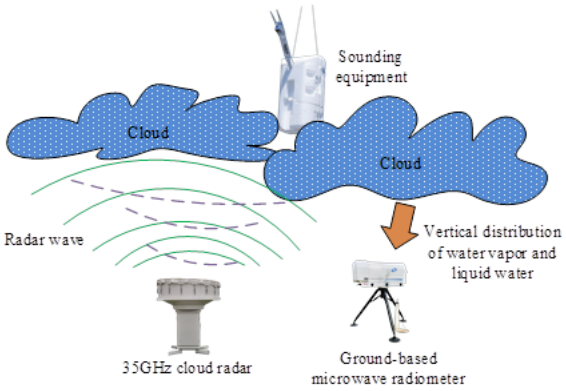

Fig. 1. Comprehensive collection system for meteorological analysis data

$$IT_{i,j} = \sum_{i=1}^{N} \sum_{j=1}^{N} \left(R_{i,j} - VPR_i\right). \tag{1}$$

In Eq. (1), $IT_{i,j}$ represents the echo intensity texture at time i and height i, $R_{i,j}$ represents the reflectivity factor at time i and height j and VPR_i represents the average profile of the reflectance factor in the time direction. The vertical variation of echo intensity is shown in Eq. (2);

$$IG_{i,j} = \sum_{i=1}^{N} \sum_{j=1}^{N} \left(R_{i,j} - VPR_j\right). \tag{2}$$

In Eq. (2), $IG_{i,j}$ represents the change in echo intensity at time i and height j. VPR_j represents the average profile of reflectance factors in the vertical direction. According to the analysis results of statistical features, data points are removed when their noise characteristics exceed the preset threshold. The median filtering method is used to further smooth the classified and preliminarily removed reflectance factor data. The median filtering calculation is shown in Eq. (3);

$$R_{filtered}\left(x, y\right) = median\left\{R(x+i, y+j)\right\}. \tag{3}$$

In Eq. (3), $R_{filtered}\left(x, y\right)$ represents the median filtering result value and (x, y) represents the median filtering window. In addition, it is necessary to carry out quality control on the brightness temperature data, which involves a lot of basic information. A quality control system for brightness temperature data is constructed, as shown in Figure 2.

As shown in Figure 2, when controlling the quality of brightness temperature data, it is necessary to combine logical checks, minimum variability checks, precipitation checks, time consistency checks, and extreme value checks. After each inspection, the data will be assigned a corresponding quality identification code, indicating the quality status of the data. If any issues are detected at any step, the data will be marked and enter the error correction process for further correction and processing. Finally, the revised data is generated and a brightness temperature quality label is generated to

ensure that the data quality meets the standard. The time consistency check requires calculating the standard deviation of meteorological elements, as shown in Eq. (4);

$$\sigma = \sqrt{\frac{1}{n}\sum_{i=1}^{n}\left(dE_t - d\bar{E}\right)^2}. \tag{4}$$

In Eq. (4), σ represents the standard deviation of meteorological elements and E_t represents the meteorological element values at time t in the time series. After obtaining meteorological data of sufficient quality, subsequent meteorological analysis can begin.

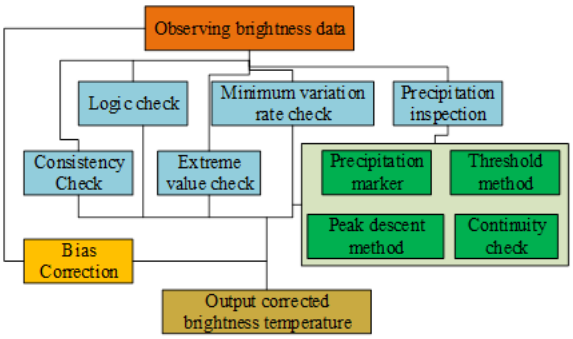

Fig. 2. Quality control system for bright temperature data

2.2. Meteorological analysis method based on computer data fusion

The atmosphere is a complex nonlinear system. The interactions between its various components cannot be simply described by linear models, making the construction and optimization of meteorological prediction models very complex. Moreover, meteorological models usually require a large amount of computing resources and have very high demands on computing power. Data fusion can improve the reliability of overall observations by combining multiple sources of data for mutual verification and correction. BP neural network can effectively capture complex nonlinear relationships between different variables, and automatically optimize their weights through training data to improve data processing efficiency and capability. On the basis of computer data fusion, a meteorological analysis method incorporating BP neural network is proposed. Before conducting meteorological analysis, it is necessary to determine the conditions for judging meteorological conditions. The relative threshold of 85% humidity is set as the boundary. Areas above the boundary are considered to have cloud cover, while areas below the boundary are considered to have no cloud cover. The BP neural network structure for meteorological analysis based on data fusion is shown in Figure 3.

As shown in Figure 3, the data input end of the network receives regional basic information collected by cloud radar and other devices. The data output terminal only sets two sets of data, relative humidity and temperature. The hidden layer is set based on the requirements of the analysis scenario, and the number of layers is determined by repeatedly combining data. Due to the fact that temperature data and humidity data belong to different categories of information, the analysis process of the two types of data is independent of each other. The number of input nodes for the temperature data section is the sum of ground temperature and humidity pressure nodes, channel brightness temperature data nodes, and cloud information nodes. The number of input nodes for the humidity data section is the number of profile layers. The number of hidden layer nodes is estimated using an empirical formula, as shown in Eq. (5):

$$n_y = \sqrt{0.42ab + 0.12b^2 + 2.54a + 0.77b + 0.35} + 0.51. \tag{5}$$

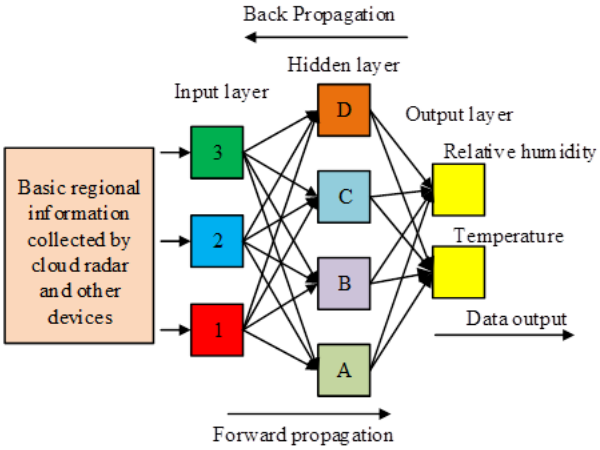

Fig. 3. BP neural network structure for meteorological analysis

In Eq. (5), n_y represents the number of hidden layer nodes, a represents the number of nodes in the input layer and b represents the number of nodes in the output layer. When transferring data between the input layer and the hidden layer, the function calculation is shown in Eq. (6):

$$\tan sig\,(n) = \frac{2}{1 + e^{-2n}} - 1. \tag{6}$$

In Eq. (6), $\tan sig\,(n)$ represents the tan-Sigmoid function and e represents the Napier constant. The neural relationship between the hidden layer and the input layer is shown in Eq. (7):

$$Y_b = \tan sig \sum_{a=1}^{L} w_{ab} X_a + B_b. \tag{7}$$

In Eq. (7), Y_b represents the hidden layer neurons, X_a represents input layer neurons, w represents the weight between two neurons and B_b represents the bias of hidden layer neurons. The neural relationship between the output layer and the hidden layer is shown in Eq. (8):

$$Z_c = \sum_{i=1}^{M} w_{bc} Y_b + B_c. \tag{8}$$

In Eq. (8), Z_c represents the output layer neuron and B_c represents the deviation of output layer neurons. The forward information transmission calculation is shown in Eq. (9):

$$int_m = \sum_{i=1}^{n} v_{im} x_i. \tag{9}$$

In Eq. (9), v_{im} represents the input layer information and int_m represents the information transmission from the input layer to the output layer. In information backpropagation, weight adjustment is performed by solving partial derivatives. The forward propagation root mean square error is expanded, as shown in Eq. (10):

$$E_z = \frac{1}{2} \sum_{n=1}^{1} \left\{ \left[y_n - f_2 \left(\sum_{n=1}^{n} w_{im} Z_m \right) \right] \right\}^2. \tag{10}$$

In Eq. (10), w_{im} represents the intermediate layer information in backpropagation, Z_m represents the last layer of information, E_z represents the forward propagation root mean square error and y_n represents the true output value of the last layer. In order to smoothly operate the meteorological analysis technology designed for research, the constructed computer model framework includes a data collection module, a data preprocessing module, a feature engineering module, a model selection and training module, a model evaluation and validation module, a visualization and result analysis module, and a deployment and monitoring module. Data collection is the starting point of the entire process, determining the quality of the foundational data for subsequent analysis. Data preprocessing and feature engineering ensure that the model is trained using clean and useful data to improve its accuracy. Model training and evaluation are the core components, ensuring the effectiveness of the selected model through scientific selection and evaluation. After completing the model training, the corresponding meteorological conditions can be obtained through information inversion analysis, as shown in Figure 4.

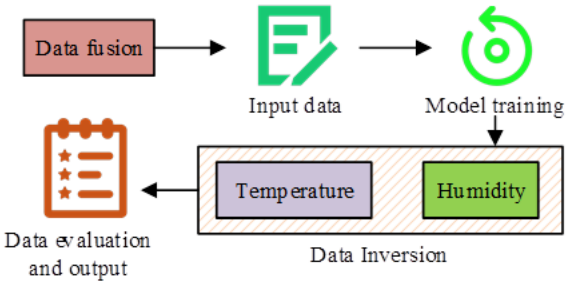

Fig. 4. The process of retrieving meteorological condition information

As shown in Figure 4, when conducting specific meteorological condition information inversion, the inversion model data that has undergone data fusion is first input. The BP neural network is trained to establish a mapping relationship from brightness temperature data to temperature and humidity profiles. In the inversion stage, the trained BP neural network inputs real-time observation data into the model. The model predicts temperature and relative humidity profiles based on these data. By comparing with actual sounding data, the effectiveness of the inversion results is evaluated. The optimized parameter details are used as the final meteorological analysis technique to analyze the input data for meteorological analysis.

3. Result

3.1. Meteorological analysis technology operational performance testing

In order to analyze the operational performance of the meteorological analysis technology designed for research, data availability and computation time are used as testing indicators. During testing, the fused data is input into the computer for processing and corresponding data information is collected. The basic software and hardware environment of the experimental equipment used is shown in Table 1.

When conducting analysis, the research method is referred to as cloud radar fusion technology. It is compared with current mainstream numerical weather prediction and data assimilation techniques. The collected data was tested for availability, as shown in Figure 5.

As shown in Figure 5, the data availability rate of different methods on different categories of data showed a decreasing trend with increasing height. In Figure 5a, in terms of humidity, the data

availability rate of numerical weather prediction was 87.2% at an altitude of 2km, and decreased to 64.9% when the altitude rose to 10km. The data availability of cloud radar fusion technology was 97.3% at an altitude of 2km, and remained above 89.0% at an altitude of 10km. As shown in Figure 5b, in terms of temperature, the data assimilation technique decreased to 77.1% when the altitude increased to 10km. The data availability of cloud radar fusion technology was 95.4% at an altitude of 2km, and remained above 85.0% at an altitude of 10km. The research method can ensure higher data availability and reduce meaningless waste of equipment resources. The calculation time of meteorological analysis results using different methods is analyzed, as shown in Figure 6.

Table 1. Basic environmental parameters of the experiment

Parameter variables	Parameter selection
Operating system	Windows10
System running memory	32GB
CPU main frequency	3.30GHz
Solid state drive space	4TB
CPU	Intel Core i5-13490
Graphics card model	NVIDIA GeForce Titan X

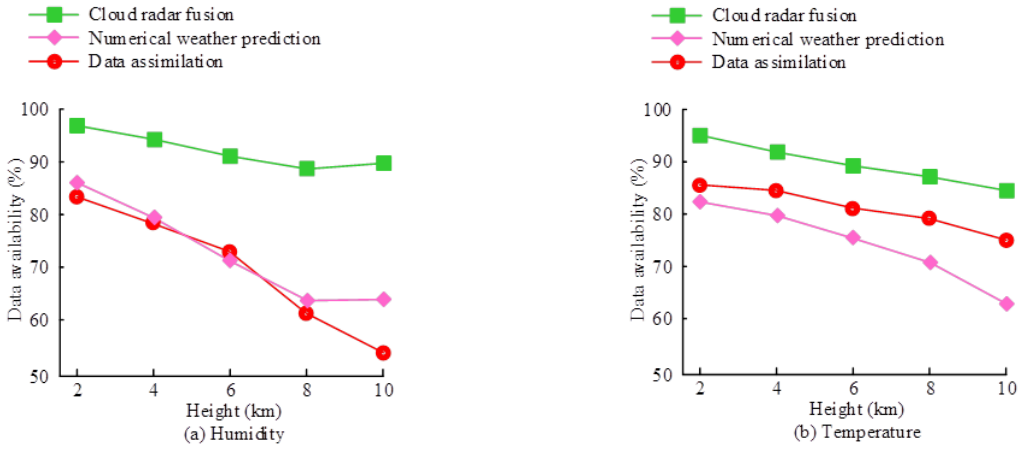

(a) humidity (b) temperature

Fig. 5. Data availability testing

As shown in Figure 6, the computation time of different methods increased with height. In Figure 6a, the calculation time for humidity data in numerical weather prediction reached over 7000ms when the altitude reached 9km. As shown in Figure 6b, the data assimilation technique took more time to calculate temperature data than humidity data when the altitude was between 4km and 7km. The humidity calculation time reached over 7000ms when the altitude reached 9km. As shown in Figure 6c, the cloud radar fusion technology maintained humidity calculation time below 6000ms and temperature calculation time below 5000ms at an altitude of 9km. This indicates that the research method as faster data analysis capability.

3.2. Application analysis of meteorological analysis technology in practical scenarios

In order to analyze the practical application effect of the research method, the research method is used for actual meteorological analysis in the range of Taiyuan ground based remote sensing vertical

observation system. The root mean square error is used to analyze the accuracy of the measured relative humidity and temperature profiles. The accuracy of the relative humidity profile is shown in Figure 7.

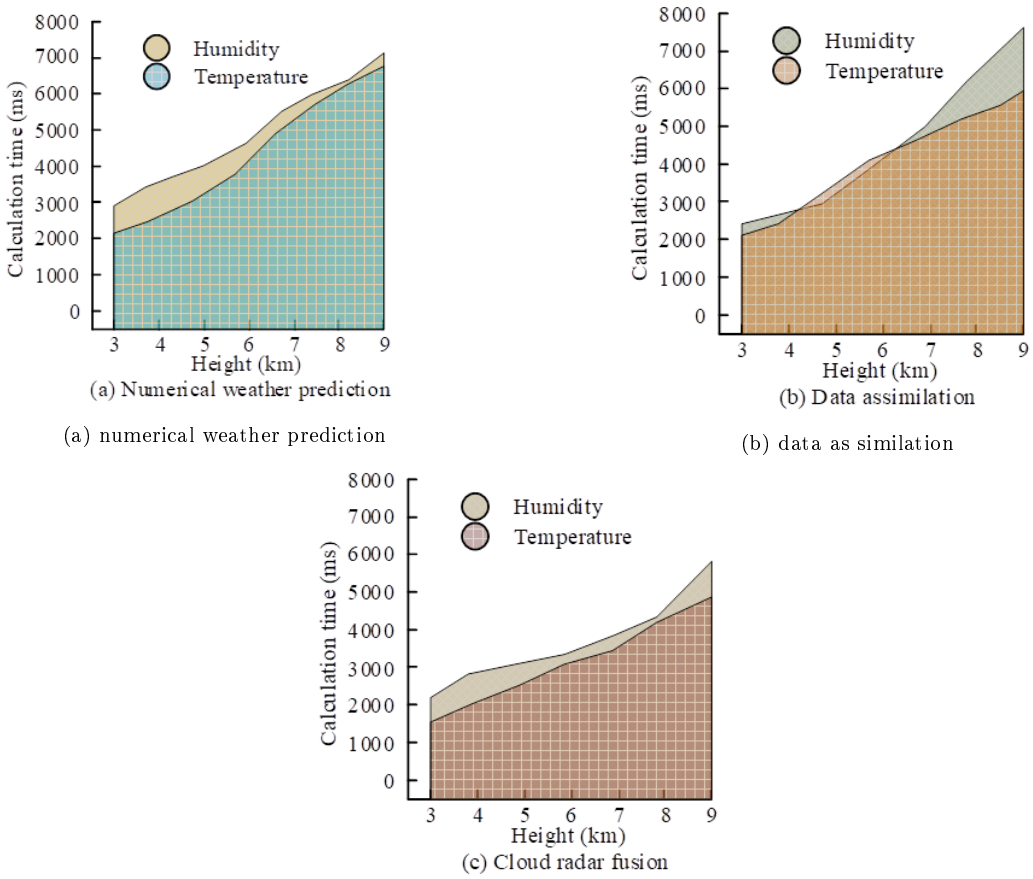

Fig. 6. Calculation time for meteorological analysis results

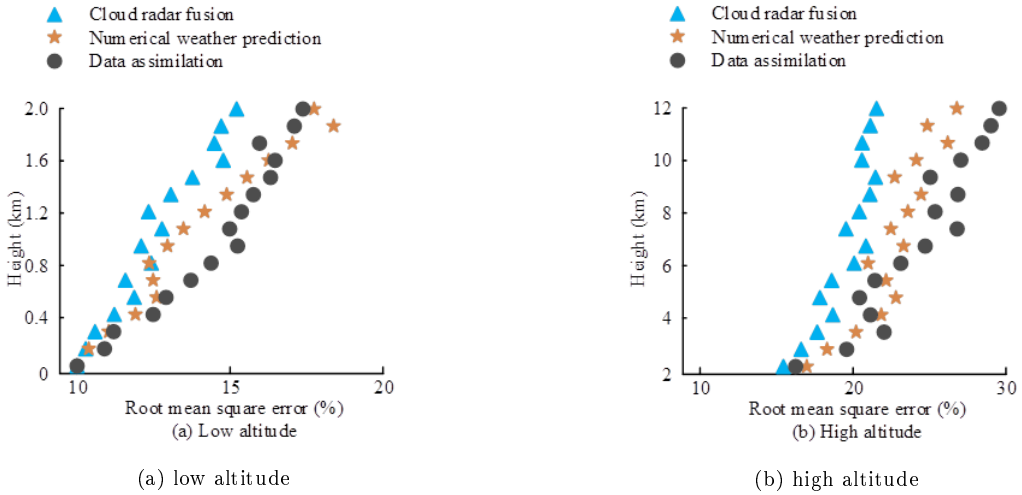

Fig. 7. Accuracy of relative humidity profile

As shown in Figure 7, the root mean square error of the relative humidity profile analyzed by different methods increased with height. In Figure 7a, in low altitude, the root mean square error of

the relative humidity profile in the numerical weather prediction reached over 18.0% as the altitude increased to 2km. When the height of cloud radar fusion technology increased to 2km, the root mean square error of the relative humidity profile was 15.4%, with significant fluctuations during the increase process. As shown in Figure 7b, at high altitudes, the root mean square error of the relative humidity profile in numerical weather prediction reached over 27.0% as the altitude increased to 12km. There was a significant pullback during the increase process, but it did not affect the overall trend. When the height increased to 12km, the root mean square error of the relative humidity profile reached over 29.0% in data assimilation technology. The cloud radar fusion technology achieved a root mean square error of 22.0% for the relative humidity profile when the height increased to 12km. However, when the height increased to 7km, the root mean square error of the relative humidity profile no longer showed a significant increasing trend. The accuracy of the temperature profile is shown in Figure 8.

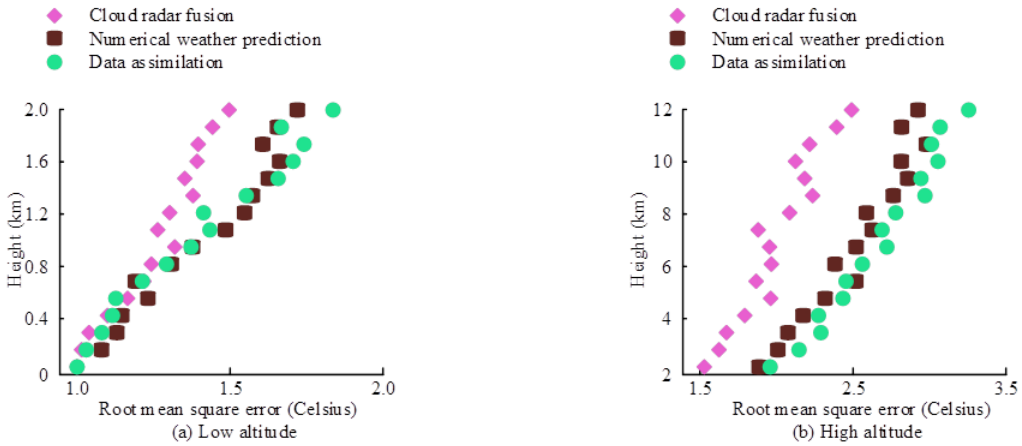

(a) low altitude (b) high altitude

Fig. 8. Accuracy of temperature profile

As shown in Figure 8, the root mean square error of the temperature profile analyzed by different method also increased with height. In Figure 8a, in low altitude, the root mean square error of the temperature profile reached over 1.9℃ when the data assimilation technique increased to an altitude of 2km. When the height increased to 2km, the root mean square error of the temperature profile in cloud radar fusion technology reached 1.5℃. As shown in Figure 8b, at high altitudes, the root mean square error of the temperature profile in numerical weather prediction reached over 3.0℃ as the altitude increased to 12km. When the height increased to 12km, the root mean square error of the temperature profile reached over 3.3℃ using data assimilation technology. When the height increased to 12km, the root mean square error of the temperature profile remained within 2.5℃ using cloud radar fusion technology. This indicates that the research method has better accuracy in meteorological analysis. The analyzed data is imported into ground based remote sensing vertical observation system to observe the effect, as shown in Figure 9.

As shown in Figure 9, after importing the meteorological analysis results into the urban observation platform, visualized images of temperature profile, relative humidity profile, and cloud particle radii were successfully generated. The temperature profile includes the pressure and temperature conditions corresponding to different time points and heights. The relative humidity profile includes the pressure and relative humidity conditions corresponding to different time points and heights. The cloud particle radius graph displays the variation of cloud particle radius at different time points

and heights. Other comprehensive performances are analyzed, as shown in Table 2.

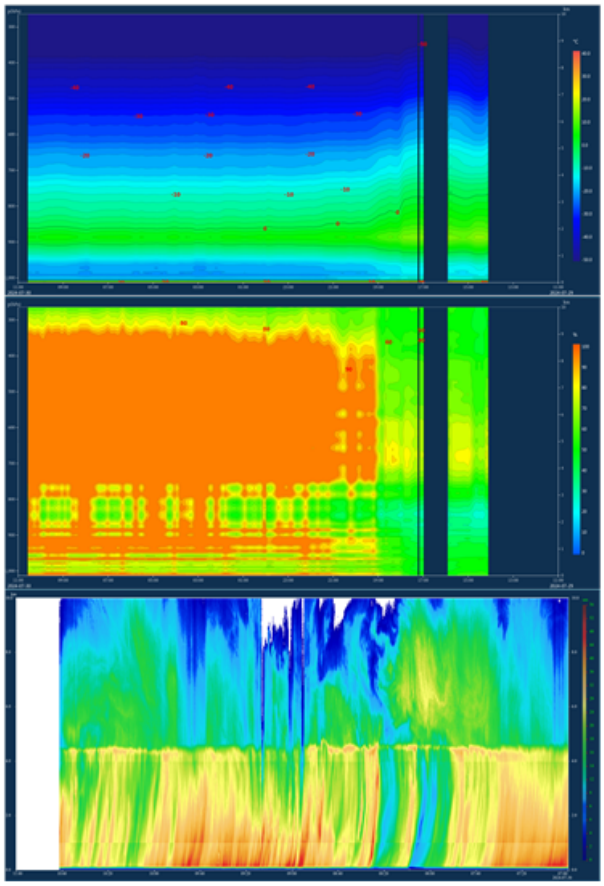

Fig. 9. Application effect of urban observation platform

Table 2. Other comprehensive performance analysis

Indicator	Cloud radar fusion	Numerical weather prediction	Data assimilation
Prediction Accuracy (%)	95.0	85.0	82.0
Model Convergence Speed (iterations)	100	150	130
Resource Utilization (%)	90.0	80.0	85.0
Data Redundancy Rate (%)	5.0	10.0	8.0
Data Processing Throughput (GB/s)	4.5	3.0	3.5
Memory Usage (%)	70.0	85.0	80.0

As shown in Table 2, among other comprehensive performance metrics, the cloud radar fusion technology had the fastest convergence speed, requiring only 100 iterations. The numerical weather prediction and data assimilation techniques required 150 and 130 iterations, respectively. The resource utilization rate of cloud radar fusion technology reached 90%, which was more efficient in utilizing hardware resources compared with the other two methods. The data processing throughput of cloud radar fusion technology reached 4.5GB/s, higher than the 3.0GB/s of numerical weather prediction and the 3.5GB/s of data assimilation technology, indicating that it could process large amounts of meteorological data more quickly. This indicates that the research method has better operational effectiveness and meteorological analysis accuracy in practical applications.

4. Conclusions

A meteorological analysis technique combining computer data fusion methods was developed for more accurate meteorological observations. A comprehensive collection system for meteorological analysis data was established based on cloud radar, generating revised data and producing brightness temperature quality indicators to ensure the data quality. A BP neural network structure was constructed for meteorological analysis based on data fusion, and corresponding meteorological conditions were obtained through information inversion analysis. The experimental results showed that when analyzing the calculation time of meteorological analysis results, the research method maintained the humidity calculation time below 6000ms and the temperature calculation time below 5000ms at an altitude of 9km. When conducting accuracy analysis of the results, the research method kept the root mean square error of the temperature profile within 2.5℃ when the height increased to 12km. The data processing throughput of the research method reached 4.5GB/s, which was higher than other methods. This indicates that the research method has stronger operational efficiency and higher accuracy in conducting meteorological analysis. However, the study does not consider the distortion of meteorological data caused by sudden natural disasters. More sudden parameters will be added to optimize the method in the future to expand the applicability of the research method.

Acknowledgement

This work was supported by Shanxi Province Meteorological Surface Project: Research on cloud physics feature inversion in Shanxi Province based on cloud radar (SXKMSDW20246752).

Conflict of interest

The authors declare that they have no conflicts of interest.

References

[1] M. R. Alizadeh and M. R. Nikoo. A fusion-based methodology for meteorological drought estimation using remote sensing data. *Remote Sensing of Environment*, 211:229–247, 2018. https://doi.org/10.1016/j.rse.2018.04.001.

[2] A. Antonini, S. Melani, M. Corongiu, S. Romanelli, A. Mazza, A. Ortolani, and B. Gozzini. On the implementation of a regional x-band weather radar network. *Atmosphere*, 8(2):25, 2017. https://doi.org/10.3390/atmos8020025.

[3] M. S. Binetti, C. Campanale, C. Massarelli, and V. F. Uricchio. The use of weather radar data: possibilities, challenges and advanced applications. *Earth*, 3(1):157–171, 2022. https://doi.org/10.3390/earth3010012.

[4] R. C. Cornes, G. Van Der Schrier, E. J. Van Den Besselaar, and P. D. Jones. An ensemble version of the e-obs temperature and precipitation data sets. *Journal of Geophysical Research: Atmospheres*, 123(17):9391–9409, 2018. https://doi.org/10.1029/2017JD028200.

[5] A. M. Dokter, P. Desmet, J. H. Spaaks, S. van Hoey, L. Veen, L. Verlinden, C. Nilsson, G. Haase, H. Leijnse, and A. Farnsworth. Biorad: biological analysis and visualization of weather radar data. *Ecography*, 42(5):852–860, 2019. https://doi.org/10.1111/ecog.04028.

[6] S. Fei, M. A. Hassan, Y. Xiao, X. Su, Z. Chen, Q. Cheng, F. Duan, R. Chen, and Y. Ma. Uav-based multi-sensor data fusion and machine learning algorithm for yield prediction in wheat. *Precision Agriculture*, 24(1):187–212, 2023. https://doi.org/10.1007/s11119-022-09938-8.

[7] P. Ferrer-Cid, J. M. Barcelo-Ordinas, J. Garcia-Vidal, A. Ripoll, and M. Viana. Multisensor data fusion calibration in iot air pollution platforms. *IEEE Internet of Things Journal*, 7(4):3124–3132, 2020. https://doi.org/10.1109/JIOT.2020.2965283.

[8] U. Germann, M. Boscacci, L. Clementi, M. Gabella, A. Hering, M. Sartori, I. V. Sideris, and B. Calpini. Weather radar in complex orography. *Remote Sensing*, 14(3):503, 2022. https://doi.org/10.3390/rs14030503.

[9] J. He, K. Yang, W. Tang, H. Lu, J. Qin, Y. Chen, and X. Li. The first high-resolution meteorological forcing dataset for land process studies over china. *Scientific Data*, 7(1):25, 2020. https://doi.org/10.1038/s41597-020-0369-y.

[10] L. Johansson, V. Epitropou, K. Karatzas, A. Karppinen, L. Wanner, S. Vrochidis, A. Bassoukos, J. Kukkonen, and I. Kompatsiaris. Fusion of meteorological and air quality data extracted from the web for personalized environmental information services. *Environmental Modelling & Software*, 64:143–155, 2015. https://doi.org/10.1016/j.envsoft.2014.11.021.

[11] N. McCarthy, A. Guyot, A. Dowdy, and H. McGowan. Wildfire and weather radar: a review. *Journal of Geophysical Research: Atmospheres*, 124(1):266–286, 2019. https://doi.org/10.1029/2018JD029285.

[12] C. Min, S. Chen, J. J. Gourley, H. Chen, A. Zhang, Y. Huang, and C. Huang. Coverage of china new generation weather radar network. *Advances in Meteorology*, 2019(1):5789358, 2019. https://doi.org/10.1155/2019/5789358.

[13] S. Park, J. Im, S. Park, and J. Rhee. Drought monitoring using high resolution soil moisture through multi-sensor satellite data fusion over the korean peninsula. *Agricultural and Forest Meteorology*, 237:257–269, 2017. https://doi.org/10.1016/j.agrformet.2017.02.022.

[14] M. Rautenhaus, M. Böttinger, S. Siemen, R. Hoffman, R. M. Kirby, M. Mirzargar, N. Röber, and R. Westermann. Visualization in meteorology—a survey of techniques and tools for data analysis tasks. *IEEE Transactions on Visualization and Computer Graphics*, 24(12):3268–3296, 2017. https://doi.org/10.1109/TVCG.2017.2779501.

[15] G. Rolph, A. Stein, and B. Stunder. Real-time environmental applications and display system: ready. *Environmental Modelling & Software*, 95:210–228, 2017. https://doi.org/10.1016/j.envsoft.2017.06.025.

[16] A. V. Ryzhkov and D. S. Zrnić. *Radar Polarimetry for Weather Observations*, volume 486. Springer, 2019. https://doi.org/10.1007/978-3-030-05093-1.

[17] E. Saltikoff, K. Friedrich, J. Soderholm, K. Lengfeld, B. Nelson, A. Becker, R. Hollmann, B. Urban, M. Heistermann, and C. Tassone. An overview of using weather radar for climatological studies: successes, challenges, and potential. *Bulletin of the American Meteorological Society*, 100(9):1739–1752, 2019. https://doi.org/10.1175/BAMS-D-18-0166.1.

[18] Z. Sokol, J. Szturc, J. Orellana-Alvear, J. Popova, A. Jurczyk, and R. Célleri. The role of weather radar in rainfall estimation and its application in meteorological and hydrological modelling—a review. *Remote Sensing*, 13(3):351, 2021. https://doi.org/10.3390/rs13030351.

[19] Q. Sun, C. Miao, Q. Duan, H. Ashouri, S. Sorooshian, and K.-L. Hsu. A review of global precipitation data sets: data sources, estimation, and intercomparisons. *Reviews of Geophysics*, 56(1):79–107, 2018. https://doi.org/10.1002/2017RG000574.

[20] S. Thorndahl, T. Einfalt, P. Willems, J. E. Nielsen, M.-C. Ten Veldhuis, K. Arnbjerg-Nielsen, M. R. Rasmussen, and P. Molnar. Weather radar rainfall data in urban hydrology. *Hydrology and Earth System Sciences*, 21(3):1359–1380, 2017. https://doi.org/10.5194/hess-21-1359-2017,2017.

[21] H. Wu, Q. Yang, J. Liu, and G. Wang. A spatiotemporal deep fusion model for merging satellite and gauge precipitation in china. *Journal of Hydrology*, 584:124664, 2020. https://doi.org/10.1016/j.jhydrol.2020.124664.

[22] S. Xu, J. Cheng, and Q. Zhang. A random forest-based data fusion method for obtaining all-weather land surface temperature with high spatial resolution. *Remote Sensing*, 13(11):2211, 2021. https://doi.org/10.3390/rs13112211.

[23] J. Yin, P. Hoogeboom, C. Unal, H. Russchenberg, F. Van Der Zwan, and E. Oudejans. Uav-aided weather radar calibration. *IEEE Transactions on Geoscience and Remote Sensing*, 57(12):10362–10375, 2019. https://doi.org/10.1109/TGRS.2019.2933912.

[24] G. Zhang, V. N. Mahale, B. J. Putnam, Y. Qi, Q. Cao, A. D. Byrd, P. Bukovcic, D. S. Zrnic, J. Gao, and M. Xue. Current status and future challenges of weather radar polarimetry: bridging the gap between radar meteorology/hydrology/engineering and numerical weather prediction. *Advances in Atmospheric Sciences*, 36:571–588, 2019. https://doi.org/10.1007/s00376-019-8172-4.